



Online xylem water isotope monitoring and soil water content profiling reveal spatial root water uptake dynamics in sunflower

Youri Rothfuss^{1,‡}, Samuel Le Gall¹, Nicolas Brüggemann¹, Sharmin Jahan¹, Mathieu Javaux², Julian Klaus³, Harry Vereecken¹, and Dagmar van Dusschoten⁴

5 ¹Institute of Bio- and Geosciences, Agrosphere (IBG-3), Forschungszentrum Jülich GmbH, Jülich, Germany

²Earth and Life Institute, Environmental Sciences (ELIE), Université catholique de Louvain, Louvain-la-Neuve, Belgium

³Department of Geography, University of Bonn, Bonn, Germany

⁴Institute of Plant Sciences (IBG-2), Forschungszentrum Jülich GmbH, Jülich, Germany

10 *Correspondence to:* Youri Rothfuss (y.rothfuss@fz-juelich.de)

Abstract. Knowledge about plant water stress regulation mechanisms (e.g., plant stem capacitance) from *in-situ* observation is crucial for the study and modeling of plant root water uptake (RWU). We present a proof of concept and a first application of a simple method for online, minimally invasive monitoring of the water stable isotopic composition of sap xylem water of *Helianthus annuus* (sunflower) by inserting a sampling tube connected to a laser spectrometer in the plant stem. After careful calibration of our method, we applied it successfully to individual sunflower plants grown in soil columns. We followed the dynamics in stem water isotopic composition in response to changing light intensity and to depth-specific, isotopically labeled water pulses. We further establish that these isotopic dynamics matched changes in RWU profiles monitored simultaneously, independently, and non-destructively by the Soil Water Profiler. We finally highlight from modeling exercises the significance of the role of plant stem capacitance: water exchanges between xylem and stem non-conducting tissues were estimated to amount to about one sixth of RWU of *Helianthus annuus*, showing that the stem itself can be expected to be a quickly accessible reservoir of water for transpiration, very similar to what is found in trees.

1 Introduction

The development of drought stress in plants arises from a discrepancy between plant atmospheric demand and root water uptake (RWU) (Javaux et al., 2013; Meinzer et al., 1993). This results in a decrease in leaf water potential, stomatal downregulation and the loss of shoot and root water, which may eventually lead to xylem failure and plant death (Mantova et al., 2022). The mechanism, by which a plant or one of its organs (e.g., stem, petiole, leaf) loses water is quantified by the so-called capacitance, i.e., the derivative of the plant (or organ) water retention function (i.e., the ratio of the changes of its water content and its water potential) and typically expressed in $\text{cm}^3 \text{ water cm}^{-3} \text{ soil MPa}^{-1}$ (Fuchs, 2025). Capacitance always occurs, but its magnitude is a function of plant water status (e.g., Campbell et al., 1979): in the absence of stressors, we typically observe cycles of water replenishment and depletion in the evening and the morning, respectively, but the daily total transpired



shoot water volume is not affected. When drought conditions prevail, replenishment does not fully occur, which leads to tissue desaturation and decrease in plant transpiration.

The implication that a plant has a hydraulic capacitance is often ignored in modeling (but see for trees, e.g., Janott et al., 2011; Sperry and Love, 2015). For herbaceous plants, modeling of xylem water flow is almost exclusively based on the concept of resistivities, which is acceptable under steady flux conditions but may be questionable under dynamic conditions or when soil becomes dry. Some experiments show that the “capacitive contribution” to the fluxes is not negligible (Li et al., 2002, Meinzer et al., 2009), and recent work, although strictly limited to laboratory conditions (for sunflower see van Dusschoten et al., 2023), indicates that the largest fraction of transpiration during drought originates from shoot water, not RWU.

The relative distribution of RWU [-] across the soil profile, may be observed from stable isotopic (^2H , ^{18}O) analysis both in the laboratory and in the field by comparing the isotopic compositions (δ) in soil layers (1..i..n) and stem (alternatively the root crown, see Barnard et al., 2006) xylem water (δ_{xyl} [-, expressed in‰]), assuming that the latter reflects that of RWU (Penna et al., 2020; von Freiberg et al., 2020; Rothfuss and Javaux, 2017):

$$\delta_{\text{xyl}} = \delta_{\text{RWU}} = \sum_{i=1}^n \delta_{\text{soil}}(i) \times \frac{q_{\text{RWU}}(i)}{Q_{\text{RWU}}} \quad (1)$$

where $q_{\text{RWU}}(i)$ [ml min^{-1}] is the uptake flow in layer i [ml min^{-1}] and Q_{RWU} [ml min^{-1}] its sum across layers (i.e., $Q_{\text{RWU}} = \sum_{i=1}^n q_{\text{RWU}}(i)$). Eq (1) relies on the assumption that the water extracted from the soil profile instantly and completely mixes inside the roots and shoot so that there is no delay between the time water is extracted and when it reaches the stem xylem. In other words, it does not consider a) potentially existing preferential connections between roots and leaves, b) the fact that conducting tissues have a certain volume, leading to a time delay, and c) the capacitance effect of the plant non-conducting tissues (and in soil as well). Some authors investigated the hypothesis of perfect mixing and explicitly considered a time delay due to sap flow transport between the uptake and the sampling location (e.g., De Deurwaerder et al., 2020). Eq. (1) also assumes no isotopic fractionation during root water uptake or during transport inside the xylem vessels.

One drawback of the isotopic methodology is that it predominantly relies on destructive sampling in the field and subsequent offline determination in the laboratory (Ceperley et al., 2024). It is also associated with well-documented uncertainties, mostly stemming from the necessity to extract water from the soil and from stem samples (Millar et al., 2022). One alternative to access δ_{xyl} is to monitor the isotopic composition of transpiration (δ_{Tr}) non-destructively with gas-exchange chambers, under the assumption – derived from mass conservation of isotopes – that δ_{Tr} equals δ_{xyl} (e.g., Knighton et al., 2020a; 2020b), and therefore can be used for retrieving root water uptake patterns:

$$\delta_{\text{Tr}} = \delta_{\text{xyl}} = \delta_{\text{RWU}} \quad (2)$$

Operating a gas-exchange chamber that encloses an entire plant may be applicable to several small crops (possibly in early growth stages) and tree saplings. However, handling is not straightforward (e.g., issues with condensation of water inside the



chamber yielding a fractionated isotopic signal). Another alternative is the direct online and continuous monitoring of δ_{xyI} , a method that is currently restricted to some deciduous and evergreen tree species (e.g., Kinzinger et al., 2025; Marshall et al., 2020; Seeger and Weiler, 2023; Volkman et al., 2016). It has revealed water transit times of several hours to days from the root system to the stem, which could point to the importance of plant capacitance. There is, however, no isotopic work studying in a holistic way the equivalences between δ_{RWU} , δ_{Tr} , and δ_{xyI} and their relationships to water stress for herbaceous plants. The objective of the present study was to provide a first proof of concept for the online monitoring of δ_{xyI} in an herbaceous individual of *Helianthus annuus* (sunflower) and to study the plant-scale response to irrigation pulses differing in their timing, location, and isotopic composition values. To achieve this objective, the sunflower stem directly above the soil surface was punctuated and the borehole connected to a laser spectrometer with a sampling tube for online measurements. Importantly, our intention was not to avoid cavitation in the xylem vessels directly impacted by the drilling as it is mandatory for direct xylem pressure measurements (see, e.g., review of Wei et al., 2001). The experiments were conducted in a hydroponics setting and in soil columns under strictly controlled conditions of temperature, humidity and light intensity in a climate chamber. Results of the isotopic monitoring were validated against those of a non-destructive, rapid, and highly precise capacitive soil volumetric water content sensor, the Soil Water Profiler (SWaP, van Dusschoten et al., 2020). Finally, the prevalence and importance of capacitance in plant water flow was evaluated with the data from two independent modeling exercises.

2 Material and methods

We conducted two independent but complementary experiments. The first experiment in hydroponic conditions (called ‘calibration experiment’ hereafter) aimed to determine the extent to which the stem water vapor collected *in situ* was isotopically representative of the xylem liquid water. More precisely, the objective was to establish ^2H - and ^{18}O -specific calibration functions to convert the stem water vapor isotopic composition ($\delta_{\text{stem}}^{\text{vap}}$) into xylem (liquid) water isotopic compositions (δ_{xyI}) values.

The second experiment (called ‘case study’ afterwards) was conducted on two potted sunflowers plants using soil columns under controlled conditions to investigate their response to irrigation pulses that differed in their soil location and timing. In this experiment, the Soil Water Profiler, SWaP (van Dusschoten et al., 2020) was used to provide independent, quantitative estimates of root water uptake profiles.

2.1 *In situ* online monitoring

$\delta_{\text{stem}}^{\text{vap}}$ was monitored by drilling a 5 mm deep and 3.5 mm diameter hole in the stem of the plants 2-3 cm above the soil surface and by connecting the borehole to a cavity ring down spectrometer (L2130-i, Picarro, Inc., Santa Clara, CA, USA) with a 1/8” diameter PTFE tubing. Thereby, at the position of the hole, the xylem is punctured and these xylem vessels will no longer contribute to xylem flow. Water vapor from the stem was passively sampled at a rate of 28 ml min⁻¹ into the PTFE tubing by the laser spectrometer. Sunflower stems contain stomata and have a leaky cuticle (Kutschera and Khanna, 2025) through which



outside air can enter stem and become water saturated. To avoid contamination of the water vapor stream in the tubing with air from the climate chamber and to prevent photosynthesis (and therefore transpiration) to happen at the sampling point (which would bias the isotopic measurement), the connection of the PTFE tubing to the plant stem was covered with a sealing paste
95 (Terostat VII, Henkel, Germany).

$\delta_{\text{stem}}^{\text{vap}}$ was calculated by averaging 1 min of collected 1 Hz continuous raw data (that is, exactly 60 data points) and correcting for the dependency of the laser spectrometer on water vapor mixing ratio (Schmidt et al., 2010). $\delta_{\text{stem}}^{\text{vap}}$ was then converted into δ_{stem} , the isotopic composition value of the liquid water transported or stored inside the stem that is at thermodynamic equilibrium with stem water vapor. For this, we used the temperature-dependent functions of Horita and Welowski (1994).
100 Finally, the δ_{stem} values were calibrated against the measurements of two in-house water vapor isotope standards, each consisting of a vessel filled with a silt loam soil (sand: 21%, silt: 66%, and clay: 13%, saturated water content: $0.45 \text{ cm}^3 \text{ cm}^{-3}$, saturated hydraulic conductivity: $1.00224 \text{ cm day}^{-1}$) and saturated with water of known isotopic composition (i.e., standard 1: $\delta^2\text{H}=-75.1\text{‰}$ and $\delta^{18}\text{O}=-14.4\text{‰}$, standard 2: $\delta^2\text{H}=69.3\text{‰}$ and $\delta^{18}\text{O}=24.7\text{‰}$). Each water vapor isotopic standard was measured once per day (see for details Deseano-Diaz et al., 2023).

105 2.2 Soil water content profiling

The Soil Water Profiler (van Dusschoten et al., 2020) consists of two ($5 \times 7 \text{ cm}^2$) Cu sheets that act as a capacitor in series with a single turn radio frequency coil thereby creating a resonator. The resonance frequency is very sensitive to the soil electric permittivity and therefore to the soil volumetric water content (SWC). As the sensor slides up and down along the soil column using a precision linear axis it functions as an online and non-destructive measurement of soil volumetric water content profiles
110 and its development over time. SWC can be determined after calibration with 8-10 soil probes of known SWC against the resonance frequency. SWC calculated in this manner has a maximum accuracy of $0.003 \text{ cm}^3 \text{ cm}^{-3}$. When combined with changing conditions in light intensity as can be done in a climate-controlled chamber, one can derive vertically resolved (cm) and high frequency (10 min) dynamics in RWU from the collected data. The main idea here is that light induces rapid changes in transpiration and xylem potential that causes quicker change in local water uptake (q_{RWU}) than in vertical (soil and plant)
115 water redistribution, which allows one to assume that the local change of water content is proportional to q_{RWU} .

2.3 Calibration experiment

To quantify the relationship between the isotopic composition measured in the stem water (δ_{stem}) and that of the stem xylem sap (δ_{xyI}), we elaborated a hydroponic settings experiment. This had the advantage of providing the plant with one single water source for root water uptake. Our working hypothesis was that, after a certain period when stem water reaches equilibrium
120 (i.e., δ_{stem} is no longer a function of time), (1) δ_{xyI} equals the isotopic composition of the hydroponic solution and (2) δ_{stem} reflects that of the hydroponic solution.

To test both hypotheses, sunflower plants were grown in aerated hydroponic solution – obtained by combining Dutch Formula GROW™ and Dutch Formula MICRO™ solutions (Advanced hydroponics of Holland, The Netherlands) in 1 ml l^{-1} and 2 ml

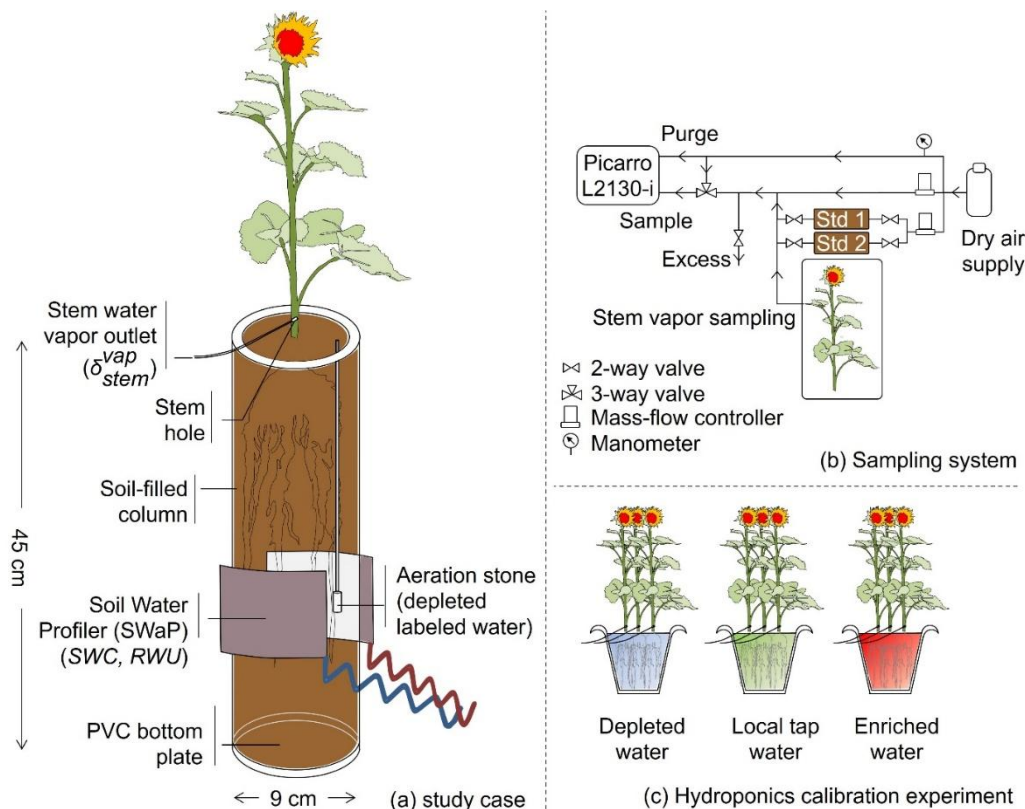


125 I^1 concentration, respectively – for a duration of three months under controlled conditions of light intensity, air temperature
(20°C) and relative humidity (50%). During that time, light intensity was set to follow a 24-hour square wave cycle, from 0
 $\mu\text{mol m}^{-2} \text{s}^{-1}$ (20:00 to 06:00) to 1200 $\mu\text{mol m}^{-2} \text{s}^{-1}$ (06:00-20:00). When the BBCH 60 vegetative stage was reached, nine plants
were removed from the hydroponic solution and placed randomly in one of three 5-l water baths (three plants per bath). Each
bath was covered with a polystyrene foam plate to prevent evaporative fractionation and to hold the plant stem; it was filled
with water of known and different isotopic composition (i.e., bath 1 (“depleted” water): $\delta^2\text{H}_{b1}=-61.8\text{‰}$ and $\delta^{18}\text{O}_{b1}=-13.6\text{‰}$,
130 bath 2 (local tap water): $\delta^2\text{H}_{b2}=-50.4\text{‰}$ and $\delta^{18}\text{O}_{b2}=-7.4\text{‰}$, and bath 3 (“enriched water”), $\delta^2\text{H}_{b3}=58.7\text{‰}$ and $\delta^{18}\text{O}_{b3}=23.5\text{‰}$).
The isotopic composition of the stem water vapor ($\delta_{\text{stem}}^{\text{vap}}$) collected from each plant was calculated (Sect. 2.1) once equilibrium
was reached (i.e., a plateau of constant isotopic composition values was observed) and the corresponding δ_{stem} was determined
at water temperature (20°C). The ^2H - and ^{18}O -specific calibration functions were obtained by comparing the isotopic
composition values in the water baths (i.e., δ_{b1} , δ_{b2} , and δ_{b3}) against the stem liquid water isotopic composition values averaged
135 across the plants in each bath (δ_{stem_b1} , δ_{stem_b2} , and δ_{stem_b3}).

2.4 Case study

2.4.1 Experimental design and environmental conditions

Two *Helianthus annuus* plants were grown each inside a PVC column (50 cm height x 9 cm diameter) filled with a loamy sand
soil (Müllers et al., 2022) packed to a dry bulk density of 1.5 kg L^{-1} (Fig. 1). Soil was packed to this density by adding 0.08
140 cm^3 of water per cm^3 soil beforehand to keep the particle size distribution homogenous across the soil profile following the
subsequent water additions during the experiment. Additional water was added until the desired SWC (mostly between 0.2
and 0.25 $\text{cm}^3 \text{cm}^{-3}$) was reached. At 30 cm depth, a porous aeration stone (Pawfly, China) was installed in the soil to allow for
depth- and isotope-specific water labeling of the soil of the two columns. The plants were placed inside a climate-controlled
chamber (air temperature: 20°C, air relative humidity: 50%) where they were watered until they reached the full flowering
145 stage (BBCH 65). During the experimental period from 06:00 to 20:00, a 4 hour-cycle of light intensity (CXA2520-0000-
000N0YN430H, Lighting Solutions, Lüdenscheid, Germany) was generated in the climate chamber, starting with two hours
of high light intensity (1000 $\mu\text{mol m}^{-2} \text{s}^{-1}$ from 06-08:00, 10-12:00 etc.) followed by two hours of low light intensity (150 μmol
 $\text{m}^{-2} \text{s}^{-1}$, from 08-10:00, 12-14:00 etc.) except for day of experiment (DoE) 2 after 10:00 in the first experiment when high light
intensity (1000 $\mu\text{mol m}^{-2} \text{s}^{-1}$) was maintained.



150

Figure 1: Experimental setups and designs: soil column and equipment used in the case study for the monitoring of the stem water vapor isotopic composition ($\delta_{\text{stem}}^{\text{vap}}$) and of the soil water content (SWC) and root water uptake (RWU) profiles with the Soil Water Profiler (SWaP) (panel a). Gas collection system and online isotopic analysis with the laser absorption spectrometer (Picarro L2130-i, Picarro Inc.) (b). Schematic of the hydroponics experiment conducted to obtain the isotopic calibration functions for the conversion to $\delta_{\text{stem}}^{\text{vap}}$ readings into δ_{soil} values (c).

155

2.4.2 Experimental timeline

A first sunflower (plant #1) with its soil column was placed into the SWaP of the climate-controlled chamber on DoE 1 at 15:10 and shortly after connection to the laser spectrometer, after which the initial conditions in volumetric water content, RWU and isotopic composition were recorded until 16:00. A second sunflower (plant#2) was placed into the climate chamber under the same light panel as plant #1. At 16:00, 16:15, and 17:00, 15, 15, and 30 ml, respectively, of isotopically enriched water ($\delta^2\text{H}=80.9\text{‰}$ and $\delta^{18}\text{O}=27.4\text{‰}$) was injected with a needle roughly 2-3 cm below the soil surface in both plant #1 and plant #2 columns. Isotopic and SWaP measurements proceeded for plant #1 overnight. On DoE 2, 15 ml of depleted water ($\delta^2\text{H}=-156.1\text{‰}$ and $\delta^{18}\text{O}=-21.5\text{‰}$) each was injected at three occasions (09:45, 10:05, and 10:15) into the aeration stones (i.e., at 30 cm depth) in both plant #1 and plant #2 columns. Measurements on plant #1 were terminated on DoE 2 at 13:50.

165

Plant #2 was placed into the SWaP on DoE 2 at 16:00, connected to the laser spectrometer to record the initial soil water content profile. Then the labeling was done, this time at the top (with enriched water) and at the bottom (with depleted water)



in a much shorter time span (i.e., 16:10-16:45) on four occasions – two for each labeled water – each time with 15 ml of water. Measurements on plant #2, and with them the experiment, were terminated on Doe 3 at 11:10.

170 Upon completion of the experiment, the soil columns were placed in a 4.7 T magnetic resonance imaging (MRI) magnet (Magnex, Oxford, UK) controlled via a MR Solutions spectrometer (Guildford, UK) to take cross-section pictures of the stems of plants #1 and #2 for assessing the impact of the drilling on the sunflower stem tissues.

2.4.3 Data analysis

For the analysis with the SWaP, the soil column was subdivided *a posteriori* into three layers: an upper layer (0-16.5 cm) encompassing the isotopically enriched water pulse, a middle layer around the aeration stone (16.5-36.5 cm) for the depleted
175 water pulse and a bottom layer (36.5-45 cm) where no labeled water was observed to enter. The fractions of the isotopically labeled pulse water can be calculated based on the known amount of present water before the pulses together with the known amounts of added water (see Appendix A for a graphical representation of the method). Furthermore, it was assumed that, within each layer the added, labeled water and the antecedent, “unlabeled” water were taken up by the roots indifferently (i.e., at the same rate) after allowing the labeled water to diffuse within the layer for at least an hour.

180 Prior to applying a pulse of isotopic labelled water, the SWC depth profile was assessed with the SWaP to calculate the contribution of non-labelled water to total RWU. After water addition, changes in the SWC profile were continuously monitored until the pulse dispersed in all three directions in the soil, which occurred within about 2 hrs, identifiable as the maximum observed local SWC in time close to the injection point. Only from that point onward could the contribution of the labeling pulse to total RWU be calculated.

185 In the second experiment, δ_{stem} was calculated with a 10-min temporal resolution, that is, by averaging the last minute (exactly 60 data points) of each consecutive 10-min period. δ_{stem} was finally converted to δ_{xy1} using the calibration equations obtained from the calibration experiment.

2.4.4 Modeling of δ_{xy1} assuming instantaneous steady-state flux conditions

δ_{xy1} was calculated using Eq. (1), considering the three layers of soil defined above (i=1: 0-16.5 cm, i=2: 16.5-36.5 cm, and
190 i=3: 36.5-45 cm):

$$\delta_{\text{xy1_calc}} = \sum_{i=1}^3 [\delta_{\text{soil}}(i) \times \text{rRWU}(i)] \quad (1\text{bis})$$

where rRWU (-) is the relative root water uptake, defined as:

$$\text{rRWU}(i) = \frac{q_{\text{RWU}}(i)}{\sum_{i=1}^3 q_{\text{RWU}}(i)} \quad (3)$$

with q_{RWU} (ml min⁻¹) the local uptake flow and determined from the time changes in soil water content profile obtained with
195 the SWaP (Sect. 2.2 and Sect. 2.4.2). Importantly, $\delta_{\text{xy1_calc}}$ could only be calculated in periods where water was extracted and



not added to the different layers. As stated above in the introduction, Eq. (1) (and therefore Eq. (1bis)) assumes that an instantaneous steady-state water flux is achieved, that is, no effect of plant hydraulic capacitance on RWU. In reality this takes longer.

Assuming no transport of water occurred across soil layers, δ_{soil} was calculated from mixing between amounts of isotopically labeled (enriched or depleted) added water (volume V_{add}) and antecedent soil water (V_{ant}) in each layer:

$$\left\{ \delta_{\text{soil}} = \frac{V_{\text{add}}}{V_{\text{tot}}} \delta_{\text{add}} + \frac{V_{\text{ant}}}{V_{\text{tot}}} \delta_{\text{ant}} \right\}_{i=1;3} \quad (4)$$

with $V_{\text{tot}} = V_{\text{add}} + V_{\text{ant}}$, the total water volume in each layer i , and where V_{ant} is calculated as the product of the soil layer volume and volumetric water content (measured by the SWaP). Finally, values for the initial soil water isotopic composition, i.e., prior to the first addition of isotopically enriched water in the upper soil layer on DoE 1 16:00-17:00, was determined – since it was not measured *in situ* during the experiment – and was assumed to be the same for both soil columns (plant #1 and plant #2). More precisely, it was computed to fall onto an evaporation line with a slope of 4‰/‰ (Rothfuss et al., 2015) and passing through the isotopic composition value of local tap water ($\delta^2\text{H} = -50.4\text{‰}$ and $\delta^{18}\text{O} = -7.4\text{‰}$) in a dual isotope ($\delta^2\text{H}$ vs. $\delta^{18}\text{O}$) plot.

2.4.5 Xylem water – stem water replacement model

A quantitative model that describes transient changes in δ_{xy1} is beyond the scope of the present study with the limited amount of data available. However, we can simulate the time needed to observe the replacement of water contained in the cortex and pith of the stem with water from the xylem upon labeling using a simple exponential model. Assuming a well-mixed stem water reservoir of effective volume V_{stem} (ml) exchanging with a fraction f_{ex} of the x xylem water flow rate Q_{RWU} , the fraction of stem water replaced r (-) follows first-order turnover kinetics, yielding (see Appendix B for a graphical representation):

$$r(t) = 1 - \exp\left(-t \cdot f_{\text{ex}} \cdot \frac{Q_{\text{RWU}}}{V_{\text{stem}}}\right) \quad (5)$$

Eq. (5) can be inverted from estimates of V_{stem} and Q_{RWU} and the time needed to reach $r=1$ from soil water content and isotopic composition data to obtain a value for f_{ex} (-), the fraction of the xylem water that exchanges with stem water. Importantly, only stem water until the drillhole location is considered here and not the water from the roots and the stem downstream of that location. We also assumed, like above (Eq. 4), that mixing of antecedent water with new, labeled water in the soil is relatively fast compared to mixing in the stem.



3 Results

3.1 Calibration experiment

More than 99.9% of the variability in isotopic composition of the hydroponic solutions was explained by a linear model of δ_{stem} – computed from the measured stem water vapor isotopic composition, $\delta_{\text{stem}}^{\text{vap}}$, and the water temperature assuming thermodynamic equilibrium conditions (see Sect. 2.1). The ^2H - and ^{18}O - linear equations obtained were:

$$\delta \text{ } ^2\text{H}_{\text{xyI}} (\text{‰}) = 1.3(\pm 0.03) \cdot \delta \text{ } ^2\text{H}_{\text{stem}} - 13.6(\pm 1.1) \quad (6a)$$

$$\delta \text{ } ^{18}\text{O}_{\text{xyI}} (\text{‰}) = 1.4(\pm 0.04) \cdot \delta \text{ } ^{18}\text{O}_{\text{stem}} - 6.7(\pm 0.5) \quad (6b)$$

with root mean square errors (RMSE) of 1.8 and 0.8‰, respectively, and where numbers in parentheses refer to standard errors of the estimated slopes and y-intercepts values (see Appendix C for the isotopic composition data feeding the linear model). The typical time needed for reaching a stable $\delta_{\text{stem}}^{\text{vap}}$ value was 20-45 minutes, that is, the time upon which antecedent water inside the stem was replaced with the new hydroponic solution. This was comparable to other *in-situ* approaches (e.g., Rothfuss et al., 2013, Beyer et al., 2020) and was independent from the magnitude of the step change in isotopic composition (i.e., the difference between initial and final $\delta_{\text{stem}}^{\text{vap}}$ value). However, results of another, separate experiment conducted in a soil pot (see Appendix D) showed that $\delta^2\text{H}$ and $\delta^{18}\text{O}$ response times were significantly shorter and were evaluated to range between 20 and 30 s, which is equal to the response time of the isotope laser spectrometer itself. We noted also that the existence of a thermodynamic equilibrium between stem water and stem water vapor at the time of sampling, a prerequisite of using the calibration functions, could be verified from the water vapor mixing ratio (WVMR) readings of the laser spectrometer. This was, on average, equal to 24340 (± 860) ppmV, yielding a relative humidity of 100% (or close to 100%) at 20°C temperature.

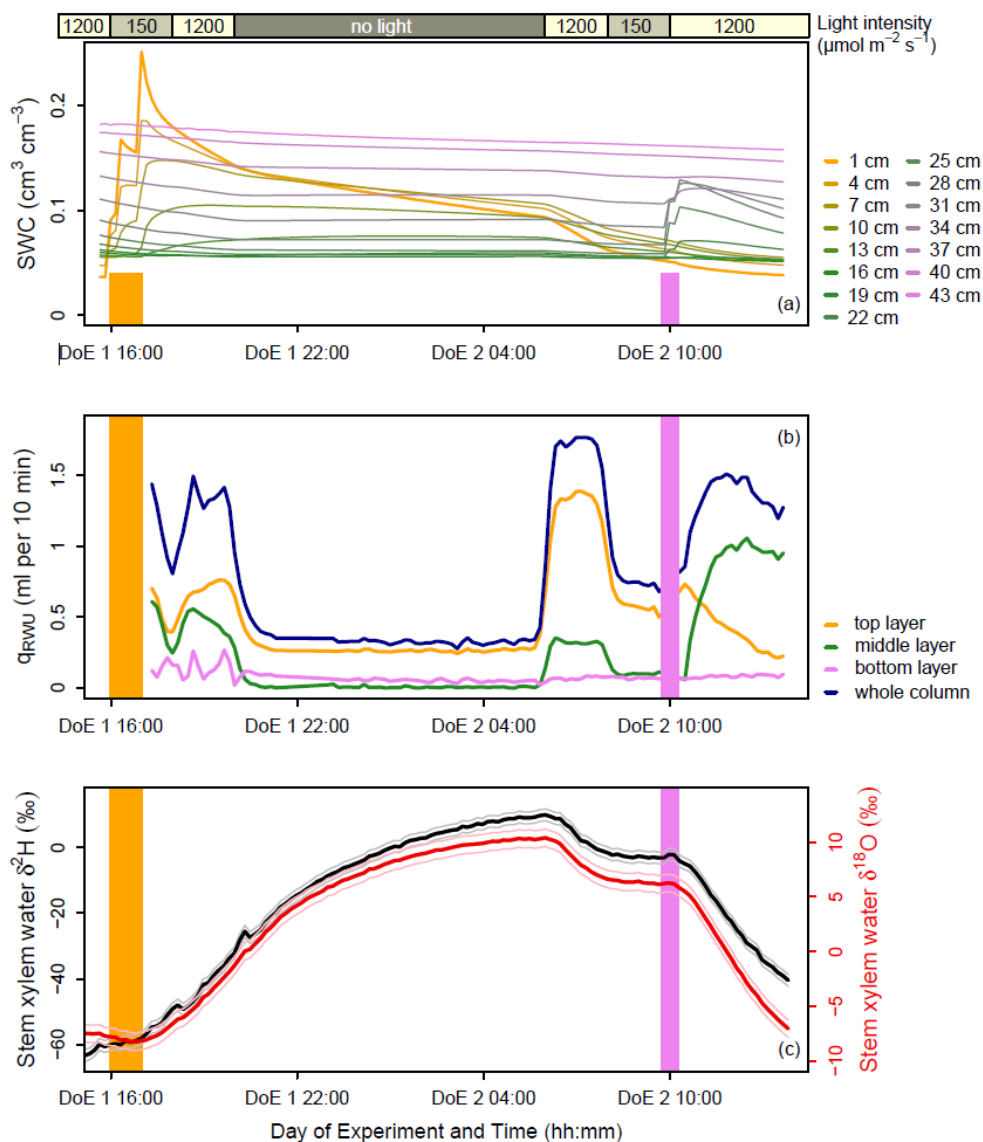
3.2 Case study: Plant responses to timing and depth of the labeling pulse

The two plants of the case study (Figs. 2 and 3) showed similar responses to the labeling pulses with some minor differences that could be explained by the timing of the pulses. Overall, there was a strong agreement between the two independent methods (isotopic *in-situ* monitoring system and SWaP) as seen from the time series of (i) soil water content (SWC) across depths (Figs 2a and 3a), of (ii) the layer (top, middle, bottom)-specific and total absolute RWU flux rate q_{RWU} and Q_{RWU} (Figs 2b and 3b), and of (iii) the (hydrogen and oxygen) isotopic composition of the stem xylem water (δ_{xyI}) obtained from calibration of the δ_{stem} observation with Eqs. (6a) and (6b) (see sections 2.3 and 3.1, Fig. 2c and 3c).

Shortly after the first enriched labeling pulse was applied to the top layer (0-16.5 cm, on DoE 1 at 16-17:00, see orange vertical stripe) of the soil of plant #1 and as the soil water content increased in that layer (Fig. 2a), the contributions to total RWU from the top and middle soil layers ($q_{\text{RWU}}^{\text{top}}$ and $q_{\text{RWU}}^{\text{mid}}$) increased and dropped, respectively (Fig. 2b, orange and green curves). Meanwhile, δ_{xyI} of plant #1 started to increase and continued increasing (at a slower time rate) after lights were switched off



250 on DoE 1 20:00 (Fig. 2c). Plant #1 xylem water did not seem to reach complete equilibrium “overnight” as δ_{xyl} reached its maximum value ($\delta^2\text{H}=10.0\text{‰}$ and $\delta^{18}\text{O}=10.4\text{‰}$) only at the end of the “night period” on DoE 2 at 06:00. As lights were turned on again, Q_{RWU} increased (from 0.33 to 1.75 ml/10 min), $q_{\text{RWU}}^{\text{top}}$ increased from 0.28 to 1.36 ml/10 min and $q_{\text{RWU}}^{\text{mid}}$ increased from 0.01 to 0.32 ml/10 min simultaneously in 50 minutes of time. This translated into a slower (~2 h) but significant (~e.g., -15‰ for $\delta^2\text{H}$) decrease in δ_{xyl} . After the addition of the second labeling pulse (DoE 2 from 09:45-10:15, violet stripe) with
255 depleted water in the middle soil layer (16.5-36.5 cm) and following the switching of the lights to high intensity (DoE 2 at 10:00) again, $q_{\text{RWU}}^{\text{top}}$ dropped significantly (0.73 to 0.22 ml/10 min) as $q_{\text{RWU}}^{\text{mid}}$ increased (from 0.06 to 0.95 ml/10 min) simultaneously. A change in δ_{xyl} was picked up concomitantly at the position of the tubing in the pith of the stem. Again, even after a few hours the isotopic composition of the xylem water had not reached equilibrium while the plant experienced high transport rates (DoE 2, 10:15-13:50). Note that, during the whole period of this first experiment, the contribution of the bottom
260 soil layer to total root water uptake remained rather constant (in average $12(\pm 6)\%$, Fig 2b).

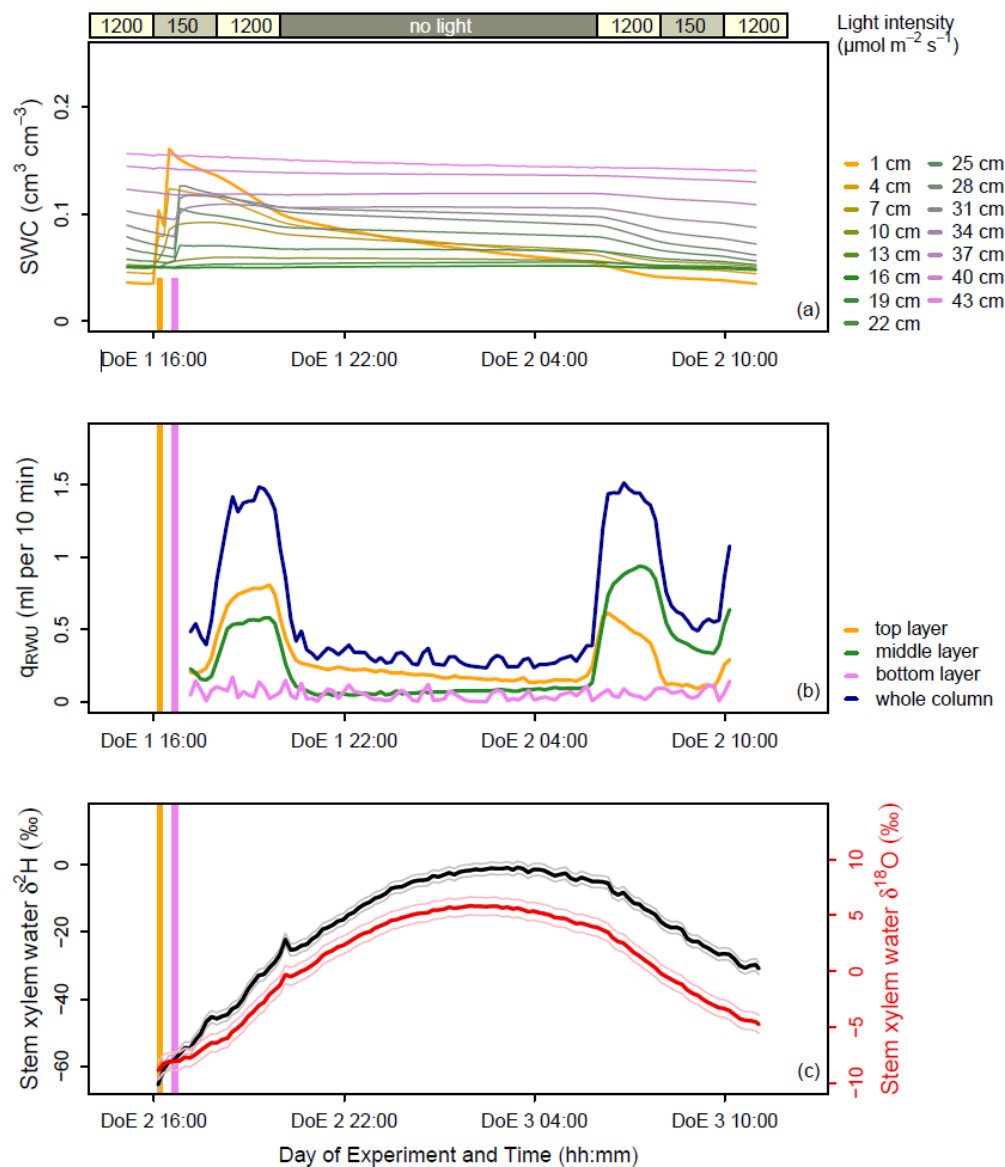


265 **Figure 2: Time courses of the soil volumetric water content (SWC, $\text{cm}^3 \text{cm}^{-3}$, panel a), the whole column and layer (top, middle, and bottom)-specific root water uptake (respectively Q_{RWU} and q_{RWU} , ml water per 10 min, panel b), and of the hydrogen (black line) and oxygen (red line) calibrated isotopic compositions of stem xylem water (δ_{xyl}) (panel c) during the case study with sunflower plant #1. δ_{xyl} was obtained from δ_{stem} online measurements and by applying the calibration functions (Eqs 6a and 6b, see section 3.1). The error in the determination of δ_{stem} is indicated on the same plot panel by the grey and light red lines for ^2H and ^{18}O , respectively. Note that SWC was measured with the Soil Water Profiler at centimeter depth-resolution but local data value is shown every three centimeters for clarity in panel (a). The orange (violet) stripes indicate the time periods when isotopically enriched (depleted) water was added to the upper (middle) soil layers of the columns. The yellow, light grey, and dark grey boxes above the plot indicate the time periods of high light intensity ($1200 \mu\text{mol m}^{-2} \text{s}^{-1}$), low light intensity ($150 \mu\text{mol m}^{-2} \text{s}^{-1}$), and where there was no light inside the climate chamber.**

270



Before the “night” (DoE 2, 20:00 to DoE 3, 06:00) of the second experiment, two labeling pulses were applied in the same order and to the same soil layers but in short succession (DoE 2 from 16:10-16:15 and from 16:35-16:45, see orange and violet stripes, Fig. 3). During the night itself, relatively more water was observed to be extracted from the middle layer in comparison to the first experiment with plant #1 (q_{RWU}^{mid} increased from 0.05 to 0.55 ml/10 min, Fig. 3b) when SWC remained more or less constant, Fig. 3a). This was associated with a lower δ_{xyl} maximum value ($\delta^2H=-0.7\text{‰}$ and $\delta^{18}O=5.9\text{‰}$) reached during the night (on DoE 3 at 03:30 and 02:00, respectively). When lights were switched on again after the night period on DoE 3 at 06:00, q_{RWU}^{mid} started to even exceed q_{RWU}^{top} , which was followed by a slightly accelerated drop in δ_{xyl} . Similarly to the earlier experiment, δ_{xyl} of plant #2 started increasing in response of the pulse and at a slower rate after the lights were switched off.



285 **Figure 3: Time courses of the soil volumetric water content (SWC, $\text{cm}^3 \text{cm}^{-3}$, panel a), the whole column and layer (top, middle, and bottom)-specific root water uptake (respectively Q_{RWU} and q_{RWU} , ml water per 10 min, panel b), and of the hydrogen (black line) and oxygen (red line) calibrated isotopic compositions of stem xylem water (δ_{xyl}) (panel c) during the case study with sunflower plant #2. δ_{xyl} was obtained from δ_{stem} online measurements and by applying the calibration functions (Eqs 6a and 6b, see section 3.1). The error in the determination of δ_{stem} is indicated on the same plot panel by the grey and light red lines for ^2H and ^{18}O , respectively. Note that SWC was measured with the Soil Water Profiler at centimeter depth-resolution but local data value is shown every three centimeters for clarity in panel (a). The orange (violet) stripes indicate the time periods when isotopically enriched (depleted) water was added to the upper (middle) soil layers of the columns. The yellow, light grey, and dark grey boxes above the plot indicate the time periods of high light intensity ($1200 \mu\text{mol m}^{-2} \text{s}^{-1}$), low light intensity ($150 \mu\text{mol m}^{-2} \text{s}^{-1}$), and where there was no light inside the climate chamber.**

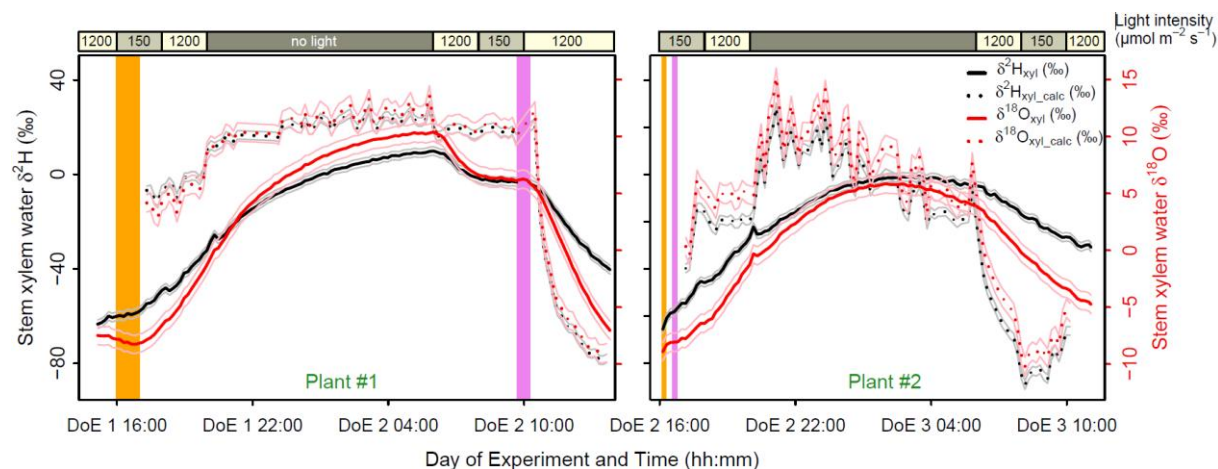
290



The differences in the magnitude of the δ_{xyI} dynamics of plant #1 and plant #2 can be linked back to the temporality of the labeling pulses. The δ_{xyI} of plant #1 reached higher values during the night from DoE 1-2 than for plant #2 because labeling with depleted (deep) water occurred only in the morning of the DoE 2 whereas both enriched and depleted water pulses were applied at the beginning of the experiment for plant #2. Consequently, plant #1 had no access to a depleted water source while it was the case for plant #2, thus yielding lower δ_{xyI} values in the latter case. Furthermore, we can infer from isotopic data that plant #2 was preferentially extracting water from the upper, enriched layer, despite having access to the lower, depleted soil water. The succession of periods, with low light intensity – high light intensity – no light intensity, had generally a more visible effect on $\delta^2\text{H}$ than on $\delta^{18}\text{O}$. In addition, while δ_{xyI} of plant #2 decreased monotonically until the end of the monitoring period (DoE 3 from 06:00 to 11:05) and did not seem to be affected strongly to changes in light intensity (DoE 3 06:00-08:00 *versus* 08:00-10:00), it was not the case for plant #1, for which the rate of decrease was (1) noticeably lower for periods of low light intensity (e.g., DoE 2, 08:00-10:00) than for periods of high light intensity (e.g., DoE 2, 10:00-16:00) and (2) higher after the labeling of the bottom of the soil (DoE 2 from 09:45-10:15). Noticeably, night-time RWU and transpiration occurred for both plants because of a vapor pressure deficit greater than zero, and the relative contribution of the uppermost layer (0-16.5 cm) to total RWU was much higher for plant #1 (in average 80(\pm 4)% from DoE 1, 20:00 to DoE 2, 06:00) than for plant #2 (in average 64(\pm 10)% from DoE 2, 20:00 to DoE 3, 06:00) – despite having access to depleted water in the bottom of the soil profile. Total RWU was always higher during the periods of high light intensity than low light intensity (Figs 2c and 3c), when excluding the periods of labeling from the analysis.

3.3 Comparison between calibrated observations and simulations of δ_{xyI}

Steady-state simulations and calibrated observations of the isotopic composition of xylem water ($\delta_{\text{xyI_calc}}$ and δ_{xyI}) showed similar trends for both investigated plants (i.e., an increase followed by a decrease), however with significant differences in the magnitude and time of the response to the labeling pulses (Fig. 4). This was, for instance, visible on DoE 2 at 06:00 when the lights were switched from 0 to 1000 $\mu\text{mol m}^{-2} \text{s}^{-1}$. While the time needed for the δ_{xyI} *in-situ* observations to reach another stable plateau of values was approximately two hours, there was an instantaneous step change in $\delta_{\text{xyI_calc}}$.



320 **Figure 4: Comparison between calibrated observations (solid lines) and simulations of the hydrogen (black color) and oxygen (red) isotopic compositions of stem xylem water (δ_{xyl}) over the courses of the 1st experiment (sunflower plant #1, left hand side) and the 2nd experiment (plant #2, right hand side). δ_{xyl} was obtained from δ_{stem} measurements and by applying the calibration functions (Eqs 6a and 6b). The error in the determination of δ_{stem} is indicated on the same plot panel by the grey and light red lines for ^2H and ^{18}O , respectively. δ_{xyl_calc} was obtained from root water uptake measurements with the Soil Water Profiler and from simulated soil water isotopic composition profiles using Eq (1bis). The orange (violet) vertical stripes indicate the time when isotopically enriched (depleted) water was added to the upper (middle) soil layers of the columns. The yellow, light grey, and dark grey boxes above the plot indicate the time periods of high light intensity, low light intensity, and where there was no light inside the climate chamber.**

325

In addition, δ_{xyl_calc} of plant #2 showed greater short-term (<0.5 h) variations than δ_{xyl_calc} of plant #1 during the “night” from DoE 2 to 3, while it was not the case for δ_{xyl} observations. Reasons for this are found in (i) a more homogeneous SWC profile for plant #2 during that night (Fig. 2c versus Fig. 3c) and in (ii) a more heterogeneous simulated water isotopic composition profile in the soil column (δ_{soil_sim}) of plant #2 (Appendix E, Tables E1 versus E2). The latter was a consequence of the third labelling event (DoE 2, 16:10-16:45) where both upper and middle layers of soil were treated (in contrast to the first and second labeling events, where only one of the two layers was treated). During nighttime, the contribution of both the upper and middle soil layers to total RWU was constant for plant #1 but not for plant #2, where the contribution of the middle layer slowly increased as the middle layer was sufficiently wetter to sustain the increased contribution (Figs. 2c versus Fig. 3c). This led to smaller measured differences in rRWU between the upper and middle layers of the soil. In other words, plant #2 could “easily” switch between the water sources contained in these two layers and these small changes in rRWU had a more important impact on plant #2- δ_{xyl_calc} than for plant #1- δ_{xyl_calc} because of marked differences in δ_{soil_sim} in the former case.

330

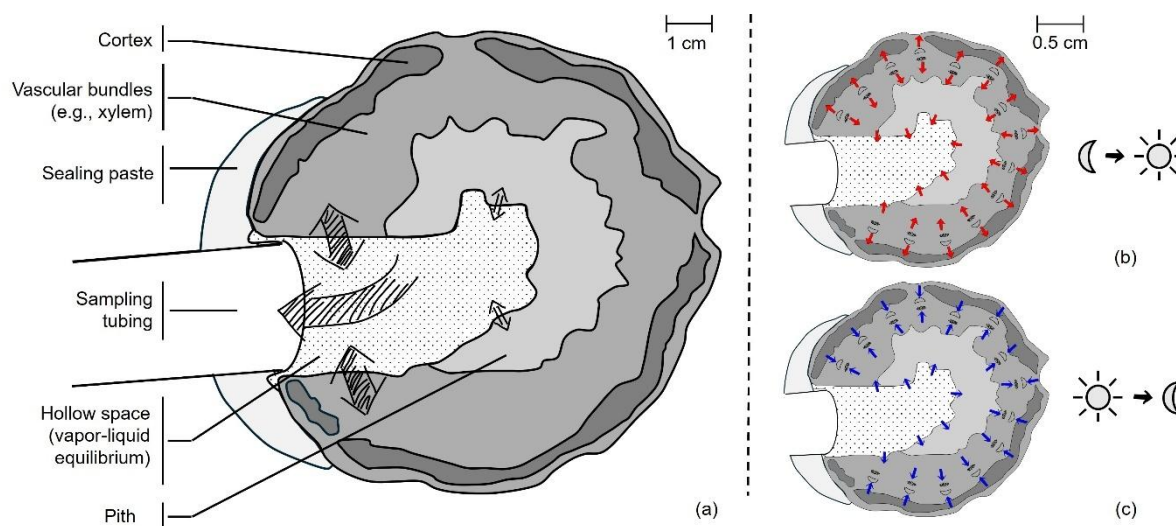
335



4 Discussion

4.1 On the difference between δ_{stem} and δ_{xtl}

The calibration experiment highlighted that (i) δ_{xtl} (i.e., by hypothesis, the isotopic composition value in the water bath in which the plant was grown) and δ_{stem} were different but (ii) the difference was the same across the nine sampled plants, and (iii) the difference was dependent on the isotopic composition value of the water bath. Our understanding is that the water vapor collected from inside the stem is in equilibrium with water from the intercellular spaces (Sifton, 1945) and xylem sap water as well as with water contained in other, non-conducting tissues (i.e., the cortex and stem center – or pith, see Fig. 5). In this regard, our *in-situ* monitoring approach resembles another destructive water vapor extraction method, namely the direct water vapor equilibrium technique (Wassenaar et al., 2008), but with a much smaller equilibration volume. Given the strong linear relationships, we believe that the contributing proportions of the non-conducting water pools to the collected stem water vapor were small. However, a definite conclusion was not possible as it would require the determination of isotopic compositions of the individual water “pools” (e.g., xylem, phloem water, parenchyma, etc.).



350 **Figure 5: Conceptual drawing of one sunflower plant stem section based on one of the magnetic resonance imaging pictures of plant #1 made after the experiment (panel a; see also Appendix F, Fig. F1). The hollow space resulting from the drilling and the installation of the sampling tubing is thought to contain water vapor equilibrated with different (liquid) water bodies contained in different stem tissues, but mainly from the vascular bundles (e.g., xylem vessel). In panels (b) and (c), situations are depicted where lights are switched from low to high intensity and from high to low intensity, respectively. In the first case (b), the opening of the stomata induces an increase in transpiration, which is initially only partly counterbalanced by an increase in root water uptake. Water is mobilized from other non-conducting tissues located in the pith and the cortex and contributes to stem water flow. In the second case (c), the closing of the stomata induces a decrease in transpiration, which is initially only partly counterbalanced by a decrease in root water uptake. Water is redistributed from the vascular bundles (e.g., xylem) back to the pith and to the cortex regions.**

360



A reason for the deviation from the $\delta_{\text{xyl}} = \delta_{\text{stem}}$ case may be found elsewhere, for instance, in possible contamination of the stem water vapor with co-sampled volatile organic compounds and spectral interference in the laser spectrometer measuring cell (Ceperley et al., 2024; Zhao et al., 2011; West et al., 2006), although a dependency of contamination to the isotopic composition value has not been observed to our knowledge. In addition, Millar et al. (2018) pointed out that the direct water vapor equilibrium technique was the least affected by organic contamination. The possibility of isotopic fractionation during root water uptake or gas diffusion from the intercellular spaces into the hollow space, or else through the epidermis via evaporation (e.g., de la Casa et al., 2022) – despite the presence of the sealing paste – may be ruled out because, as stated above, the $\delta_{\text{xyl}} - \delta_{\text{stem}}$ deviation was not constant across the tested isotopic composition range (whereas isotopic fractionation should be isotopic composition-independent). Finally, it could be proved (i.e., by flushing dry synthetic air in the direct vicinity of the connection and observing no effect on the water vapor mixing ratio readings of the laser spectrometer) that contamination of the sampled stem water vapor with climate chamber air was prevented by sealing the tubing-stem connection. However, the stem remains quite porous (see MRI pictures in Appendix F, Fig. 1) so air should infiltrate into the stem, potentially upstream of the sampling location.

To be complete, calibration should be performed at other key growth stages and memory effects should be specifically investigated. The calibration functions should be redetermined from inflorescence emergence (BBCH 50-59) to fruit development (BBCH 70-79), that is, as soon as the stem can hold the 1/8” sampling tubing. In addition, further experiments should include different isotopic trajectories of the stem water, i.e., with different initial conditions (hydroponic solution water isotopic composition) for the same end conditions (water bath isotopic composition) to investigate possible memory effects. Calibration could also include the destructive sampling (and further laboratory extraction with, e.g., the cryogenic vacuum distillation technique, Orłowski et al., 2018) of the sunflower stem at the sampling point (where the PTFE tubing is connected to the plant) once the *in-situ* measurement is complete and the collected water vapor plant has reached equilibrium. We should finally extend the calibration experiment to sunflowers planted in soil columns to verify that the differences in environmental settings (hydroponic solution *versus* soil) did not yield significant differences in characteristics (magnitude, time) of the responses to the labeling pulses during the case study.

385 4.2 On the difference between calibrated observations and steady-state simulations of δ_{xyl}

First, the computation of $\delta_{\text{xyl_calc}}$ required that the rRWU data determined with the SWaP and used in Eq. (1bis) was affected by small errors. Further, Eq (1bis) (and therefore (1)) is built on simplifying assumptions: it implies that (1) the plant extracts from the isotopically labeled water and the soil antecedent water indifferently, (2) the water extracted across the soil profile instantly and completely mixes inside the root system and the stem so that there is no delay between the time water is extracted and when it reaches the stem xylem at the position of the tubing, in other words, the role of the plant capacitance is overlooked, (3) there is no isotopic fractionation during root water uptake or during transport inside the xylem vessels.

Our calculations show faster changes in $\delta_{\text{xyl_calc}}$ than what was determined from measurements after calibration (δ_{xyl}), however with observed values near to equilibrium (i.e., at the end of the “night” periods in both experiments) rather close to our



calculations. Main differences were found in response times between the theoretical case of a plant without an internal water
395 volume and the practical case, where water mixes with a delay inside the root and stem. As depicted in Fig. 5b and c,
assumption (2) above would explain short-term $\delta_{\text{xyI_calc}} - \delta_{\text{xyI}}$ deviations following changes in light intensity. For example, when
lights are switched from low to high intensity, the almost instantaneous increase in leaf transpiration due to stomata opening
is not counterbalanced by an increase in RWU right away, which leads mechanically to an extraction of water from the stem
(i.e., dehydration of the stem) starting with the water closest to the xylem, which probably holds the highest concentration of
400 isotopically labelled water. This can be deduced from the observation that the xylem water isotopic composition has not
reached its maximum yet at the end of the night (e.g., plant #1). Therefore, the change in relative contributions of root water
and stem water to transpiration flow is associated with a change in isotopic composition, especially in the context of labeling.
Finally, $\delta_{\text{xyI_calc}}$ is also sensitive to the initial conditions in soil water isotopic composition prior the first labeling (DoE 1 at
16:00, see Appendix E), which was not measured *in situ* but simulated as well.

405 4.3 Role of plant capacitance in RWU

Drilling the hole in the stem damages xylem vessels and disrupts xylem water flow in affected vessels. Our method cannot
directly track the isotopic composition of xylem water (δ_{xyI}), rather that of stem water (δ_{stem}), in our case mostly pith water
(Fig. 5a). Our results show that δ_{stem} changed over time, which can only mean that xylem water from undamaged vessels was
in exchange with pith water. This implies that stem water capacitance delays the signal observed with our method. This
410 observation is furthermore in line with our SWaP results where we can observe that uptake patterns shift rapidly upon the
addition of the labeling pulses, whereas changes in δ_{stem} are significantly slower.

The reduction of RWU in the middle layers upon labelling of the top layer in the first experiment implies that the added water
gets in contact with roots rapidly as otherwise no reduction in RWU in the lower layer is possible (see green line in Fig. 2b).
Even though we cannot instantaneously quantify RWU from layers where water is added, as it takes some time before the
415 added water reaches the sample tubing height from the pulse location, this observation of reduced uptake elsewhere is positive
proof that the pulse has arrived at roots, and we may expect δ_{xyI} and therefore δ_{stem} to rise afterwards. At the tubing position in
the stem, the rise of the water isotopic composition is not as rapid as the change that we would observe in the roots. It should
also be noted here that ^2H can exchange with solid phase protons, especially those of the C-OH groups abundant in
carbohydrates. This may cause a slower change in stem water $\delta^2\text{H}$ than $\delta^{18}\text{O}$.

420 Based on the SWaP data we know how much water passed through the stem per hour ($Q_{\text{RWU}} \sim 3 \text{ ml h}^{-1}$). Further, the volume
of the stem from which we sampled the water vapor can be roughly estimated from its diameter ($\sim 2 \text{ ml}$). If $f_{\text{ex}}=1$ is set in the
simple replacement model (Eq. 5), that is, all water flowing in the xylem is isotopically exchanging with water from the (non-
conducting) stem tissues, stem water would reach a constant δ_{stem} in roughly 2 h. On the other hand, if $f_{\text{ex}}=1/6$, it would take
10 h for stem water to be replaced nearly fully with the xylem water, which would be roughly in line with our observation for
425 plant #1. As it takes time for water to diffuse in the soil and later from the xylem to the sampling point during which it can
exchange with the surrounding tissue, f_{ex} gives us an estimated minimal exchange fraction of xylem flow rate of about a sixth



of RWU, which clearly is non-negligible. Ignoring the first step above results in an overestimation of f_{ex} as the inflow of isotopologues takes time to rise in the xylem of the roots. Ignoring the second step, i.e., the diffusion into the stem and later into the sampled air space, also takes time, but would result in an underestimation of f_{ex} . Even though at the current stage
430 quantification of local stem capacitance was not possible, this combination of methods should in principle allow calculating the capacitance of stems of herbaceous plants that may provide valuable new information that is not easily accessible with other methods (water potential measurements in combination with relative water content measurements, Bartlett, 2012). Furthermore, the combination provides valuable insights into the dynamics of both RWU and its relation to exchange in plant stem water content. When so much of the xylem water exchanges continuously with the stem, the stem itself can be expected
435 to be a quickly accessible reservoir of water for transpiration, very similar to what is found in trees (Preisler et al., 2022) and may very well be non-negligible during drought.

Our data shows that the isotopic composition of water in aboveground tissues should not be approached as if there is a static distribution of belowground water reservoirs, but more like a dynamic relative water availability profile that depends on the climatic demand. That is, light changes cause a change in the RWU profile especially when soil dries out (van Dusschoten et al., 2020, Müllers et al., 2023), which has a dynamic effect on the stem water isotopic composition. When the reservoir of the
440 stem is quite large relative to the xylem flow rate, changes in the stem isotopic composition will be expected to be very low, and it is important that this factor is considered when performing in-field studies, especially for larger woody species, as was pointed out by, e.g., Fabiani et al. (2022) and Barbeta et al. (2021).

4.4 Sensitivity to, impacts of, and long-term applicability of the *in-situ* monitoring method

445 The method showed to be sensitive to the insertion depth of the PTFE sampling tubing inside the stem and to the installation height above the soil surface. To work, the tubing had to be inserted (i) only a couple of millimeters inside the stem and (ii) close to the root crown. Failure to do so resulted in invalid data during the experiments, e.g., the WVMR was either too low or too high – the latter pointing to the presence of liquid water inside the sample tubing because of a direct contact with the wet (pith) tissue.

450 While the impact of the drilling on the different stem tissues was visible according to the magnetic resonance imaging (MRI) stereomicroscopic section pictures of plants #1 and #2 (see possible drying patterns, Appendix F, Fig. F1), no plant showed visible signs of stress during both the calibration experiment and the case study. Other independent pre-tests (not described here) indicated that monitoring could be practically done for 96 hours continuously. A long-term application is yet to be conducted to test possible restrictions of the method linked to the health of the plant, aging of the hole, or to plant defense
455 mechanisms leading to the sealing of the hole. Note that the monitoring method was tested with a 1/16" diameter tubing with the objectives of (i) minimizing the effects of the invasive installation and (ii) allowing monitoring at earlier growth stages (i.e., when the stem diameter is too small for a 1/8" diameter tubing). The tests were, however, not conclusive: the WVMR did not stabilize, and condensation occurred systematically inside the tubing.



5 Conclusion and outlook

460 In this work, we provided a proof of concept and a first application of a simple method to monitor the isotopic composition of
xylem sap water in a non-woody plant species under controlled conditions. Our method proved to be efficiently calibratable
($R^2=99.9\%$) and statistically reproducible in an initial hydroponics experiment. The case study showed that the method also
provided consistent results, both from a theoretical standpoint and by comparison with another, independent non-destructive
observation technique, the Soil Water Profiler. The combination of these methods also provided valuable insights into the role
465 of the stem capacitance in the RWU process, that is, the relation between the extracted water and stem water. With some
further improvements in methodology and data analysis, the combined approach should help improve our understanding of
stand-alone isotopic studies for determination of plant water use that are typically based on destructive sampling.

The method should open avenues in the study of the role of plant capacitance on RWU, and generally in the study of residence
and transit time of water in plants (e.g., like it is usually done on basis of water stable isotopic data for watersheds; Benettin et
470 al., 2022), notably through the comparison between the isotopic composition of xylem water to that of transpiration (measured
from gas-exchange chamber). We encourage the community to consider such an approach for other plant species and under
various environmental (e.g., field) conditions (albeit after careful specific calibration, e.g., in hydroponic solution) as it can be
applied quite easily, that is, without the need for specific materials or equipment other than the laser spectrometer and a power
source.

475 Data availability

Data is made available by the authors on request.

Author contributions

YR and DvD: conceptualization, methodology, investigation, formal analysis, visualization, writing – original draft
preparation, writing – review & editing, funding acquisition, supervision. SLG: methodology, investigation, formal analysis,
480 visualization, writing – review & editing, supervision. SJ: investigation, formal analysis. NB and HV: writing – review &
editing, funding acquisition. MJ and JK: writing – review & editing.

Competing interests

The authors declare that they have no conflict of interest.



Acknowledgements

485 The authors would like to thank Beate Uhlig, Johannes Kochs and Daniel Pflugfelder from the Institute of Plant Sciences (IBG-2) and Sirgit Kummer and Holger Wissel from the Institute of Bio- and Geosciences – Agrosphere (IBG-3) of the Research Center in Jülich.

Financial support

This study was conducted in the framework of and with means from the Bioeconomy Portfolio Theme of the Helmholtz
490 Association of German Research Centers.

References

- Barbeta, A., Burlett, R., Martín-Gómez, P., Fréjaville, B., Devert, N., Wingate, L., Domec, J. C., and Ogée, J.: Evidence for distinct isotopic compositions of sap and tissue water in tree stems: consequences for plant water source identification. *New Phytol.*, 233(3), 1121-1132, <https://www.doi.org/10.1111/nph.17857>, 2022.
- 495 Barnard, R. L., de Bello, F., Gilgen, A. K., and Buchmann, N.: The $\delta^{18}\text{O}$ of root crown water best reflects source water $\delta^{18}\text{O}$ in different types of herbaceous species. *Rapid Commun. Mass Spectrom.*, 20(24), 3799-3802, <https://www.doi.org/10.1002/rcm.2778>, 2006.
- Bartlett, M. K., Scoffoni, C., and Sack, L.: The determinants of leaf turgor loss point and prediction of drought tolerance of species and biomes: a global meta-analysis. *Ecol. Lett.*, 15(5), 393-405, <https://www.doi.org/10.1111/j.1461-0248.2012.01751.x>, 2012.
- 500 Benettin, P., Rodriguez, N. B., Sprenger, M., Kim, M., Klaus, J., Harman, C. J., van der Velde, Y., Hrachowitz, M., Botter, G., McGuire, K. J., Kirchner, J. W., Rinaldo, A., and McDonnell, J. J.: Transit Time Estimation in Catchments: Recent Developments and Future Directions. *Water Resour. Res.*, 58(11), e2022WR033096, <https://www.doi.org/10.1029/2022WR033096>, 2022.
- 505 Beyer, M., Kühnhammer, K., and Dubbert, M.: In situ measurements of soil and plant water isotopes: a review of approaches, practical considerations and a vision for the future. *Hydrol. Earth Syst. Sc.*, 24(9), 4413-4440, <https://www.doi.org/10.5194/hess-24-4413-2020>, 2020.
- Campbell, G. S., Papendick, R. I., Rabie, E., and Shayongowi, A. J.: Comparison of Osmotic Potential, Elastic-Modulus, and Apoplastic Water in Leaves of Dryland Winter-Wheat. *Agron. J.*, 71(1), 31-36, <https://www.doi.org/10.2134/agronj1979.00021962007100010008x>, 1979.
- 510 Ceperley, N., Gimeno, T. E., Jacobs, S. R., Beyer, M., Dubbert, M., Fischer, B., Geris, J., Holko, L., Kuebert, A., Le Gall, S., Lehmann, M. M., Llorens, P., Millar, C., Penna, D., Prieto, I., Radolinski, J., Scandellari, F., Stockinger, M., Stumpp, C., Tetzlaff, D., van Meerveld, I., Werner, C., Yildiz, O., Zuecco, G., Barbeta, A., Orłowski, N., and Rothfuss, Y.: Toward a



- common methodological framework for the sampling, extraction, and isotopic analysis of water in the Critical Zone to study
515 vegetation water use. Wiley Interdisciplinary Reviews-Water, 11(4), <https://www.doi.org/10.1002/wat2.1727>, 2024.
- Couvreur, V., Vanderborght, J., and Javaux, M.: A simple three-dimensional macroscopic root water uptake model based on
the hydraulic architecture approach. Hydrol. Earth Syst. Sc., 16(8), 2957-2971, <https://www.doi.org/10.5194/hess-16-2957-2012>, 2012.
- De Deurwaerder, H. P. T., Visser, M. D., Detto, M., Boeckx, P., Meunier, F., Kuehnhammer, K., Magh, R. K., Marshall, J. D.,
520 Wang, L. X., Zhao, L. J., and Verbeeck, H.: Causes and consequences of pronounced variation in the isotope composition of
plant xylem water. Biogeosciences, 17(19), 4853-4870, <https://www.doi.org/10.5194/bg-17-4853-2020>, 2020.
- De la Casa, J., Barbata, A., Rodríguez-Uña, A., Wingate, L., Ogée, J., and Gimeno, T. E.: Isotopic offsets between bulk plant
water and its sources are larger in cool and wet environments. Hydrol. Earth Syst. Sc., 26(15), 4125-4146,
<https://www.doi.org/10.5194/hess-26-4125-2022>, 2022.
- 525 Diaz, P. A. D., van Dusschoten, D., Kübert, A., Brüggemann, N., Javaux, M., Merz, S., Vanderborght, J., Vereecken, H.,
Dubbert, M., and Rothfuss, Y.: Response of a grassland species to dry environmental conditions from water stable isotopic
monitoring: no evident shift in root water uptake to wetter soil layers. Plant Soil, 482(1-2), 491-512,
<https://www.doi.org/10.1007/s11104-022-05703-y>, 2023.
- Fabiani, G., Penna, D., Barbata, A., and Klaus, J.: Sapwood and heartwood are not isolated compartments: Consequences for
530 isotope ecohydrology. Ecohydrology, 15(8), <https://www.doi.org/10.1002/eco.2478>, 2022.
- Fricke, W.: Night-Time Transpiration - Favouring Growth? Trends Plant Sci., 24(4), 311-317,
<https://www.doi.org/10.1016/j.tplants.2019.01.007>, 2019.
- Fuchs, M.: Revealing the Hidden Role of Capacitance in the Water Flow Through Plants to the Atmosphere. Plant Cell Environ,
48(5), 3217-3224, <https://www.doi.org/10.1111/pce.15343>, 2025.
- 535 Horita, J. and Wesolowski, D. J.: Liquid-Vapor Fractionation of Oxygen and Hydrogen Isotopes of Water from the Freezing
to the Critical-Temperature. Geochim. Cosmochim. Acta, 58(16), 3425-3437, [https://www.doi.org/10.1016/0016-7037\(94\)90096-5](https://www.doi.org/10.1016/0016-7037(94)90096-5), 1994.
- Hübner, G.: Zum Wassertransport in *Vicia faba*. Flora oder Allgemeine Botanische Zeitung, 148(4), 549-594,
[https://www.doi.org/10.1016/S0367-1615\(17\)33175-0](https://www.doi.org/10.1016/S0367-1615(17)33175-0), 1960.
- 540 Janott, M., Gayler, S., Gessler, A., Javaux, M., Klier, C., and Priesack, E.: A one-dimensional model of water flow in soil-
plant systems based on plant architecture. Plant Soil, 341(1-2), 233-256, <https://www.doi.org/10.1007/s11104-010-0639-0>,
2011.
- Javaux, M., Couvreur, V., Vanderborght, J., and Vereecken, H.: Root Water Uptake: From Three-Dimensional Biophysical
Processes to Macroscopic Modeling Approaches. Vadose Zone J., 12(4), <https://www.doi.org/10.2136/vzj2013.02.0042>, 2013.
- 545 Kinzinger, L., Haberstroh, S., Mach, J., Weiler, M., Orlowski, N., and Werner, C.: Continuous In-Situ Water Stable Isotopes
Reveal Rapid Changes in Root Water Uptake by *Fagus sylvatica* During Severe Drought. Plant Cell Environ, 48(10), 7627-
7639, <https://www.doi.org/10.1111/pce.70055>, 2025.



- Knighton, J., Singh, K., and Evaristo, J.: Understanding Catchment-Scale Forest Root Water Uptake Strategies Across the Continental United States Through Inverse Ecohydrological Modeling. *Geophys. Res. Lett.*, 47(1), e2019GL085937, 550 <https://www.doi.org/10.1029/2019GL085937>, 2020.
- Knighton, J., Kuppel, S., Smith, A., Soulsby, C., Sprenger, M., and Tetzlaff, D.: Using isotopes to incorporate tree water storage and mixing dynamics into a distributed ecohydrologic modelling framework. *Ecohydrology*, 13(3), e2201, <https://www.doi.org/10.1002/eco.2201>, 2020.
- Kübert, A., Dubbert, M., Bamberger, I., Kühnhammer, K., Beyer, M., van Haren, J., Bailey, K., Hu, J., Meredith, L. K., Ladd, 555 S. N., and Werner, C.: Tracing plant source water dynamics during drought by continuous transpiration measurements: An in-situ stable isotope approach. *Plant Cell Environ*, 46(1), 133-149, <https://www.doi.org/10.1111/pce.14475>, 2023.
- Kühnhammer, K., Kübert, A., Brüggemann, N., Diaz, P. D., van Dusschoten, D., Javaux, M., Merz, S., Vereecken, H., Dubbert, M., and Rothfuss, Y.: Investigating the root plasticity response of *Centaurea Jacea* to soil water availability changes from isotopic analysis. *New Phytol.*, 226(1), 98-110, <https://www.doi.org/10.1111/nph.16352>, 2020.
- 560 Kutschera, U. and Khanna, R.: Stomatal development and epiphytic bacteria in sunflower hypocotyls. *Plant Signaling & Behavior*, 20(1), 2548312, <https://www.doi.org/10.1080/15592324.2025.2548312>, 2025.
- Li, Y., Fuchs, M., Cohen, S., Cohen, Y., and Wallach, R.: Water uptake profile response of corn to soil moisture depletion. *Plant Cell Environ*, 25(4), 491-500, <https://www.doi.org/10.1046/j.1365-3040.2002.00825.x>, 2002.
- Mantova, M., Cochard, H., Burrell, R., Delzon, S., King, A., Rodriguez-Dominguez, C. M., Ahmed, M. A., Trueba, S., and 565 Torres-Ruiz, J. M.: On the path from xylem hydraulic failure to downstream cell death. *New Phytol.*, 237(3), 793-806, <https://www.doi.org/10.1111/nph.18578>, 2023.
- Marshall, J. D., Cuntz, M., Beyer, M., Dubbert, M., and Kuehnhammer, K.: Borehole Equilibration: Testing a New Method to Monitor the Isotopic Composition of Tree Xylem Water. *Front Plant Sci*, 11, 358, <https://www.doi.org/10.3389/fpls.2020.00358>, 2020.
- 570 Meinzer, F. C.: Stomatal Control of Transpiration. *Trends Ecol. Evol.*, 8(8), 289-294, [https://www.doi.org/10.1016/0169-5347\(93\)90257-P](https://www.doi.org/10.1016/0169-5347(93)90257-P), 1993.
- Meinzer, F. C., Johnson, D. M., Lachenbruch, B., McCulloh, K. A., and Woodruff, D. R.: Xylem hydraulic safety margins in woody plants: coordination of stomatal control of xylem tension with hydraulic capacitance. *Funct. Ecol.*, 23(5), 922-930, <https://www.doi.org/10.1111/j.1365-2435.2009.01577.x>, 2009.
- 575 Millar, C., Pratt, D., Schneider, D. J., and McDonnell, J. J.: A comparison of extraction systems for plant water stable isotope analysis. *Rapid Commun. Mass Spectrom.*, 32(13), 1031-1044, <https://www.doi.org/10.1002/rcm.8136>, 2018.
- Millar, C., Janzen, K., Nehemy, M. F., Koehler, G., Hervé-Fernández, P., Wang, H. X., Orlowski, N., Barbeta, A., and McDonnell, J. J.: On the urgent need for standardization in isotope-based ecohydrological investigations. *Hydrol. Process.*, 36(10), e14698, <https://www.doi.org/10.1002/hyp.14698>, 2022.



- 580 Müllers, Y., Postma, J. A., Poorter, H., Kochs, J., Pflugfelder, D., Schurr, U., and van Dusschoten, D.: Shallow roots of different crops have greater water uptake rates per unit length than deep roots in well-watered soil. *Plant Soil*, 481(1-2), 475-493, <https://www.doi.org/10.1007/s11104-022-05650-8>, 2022.
- Orlowski, N., Breuer, L., Angeli, N., Boeckx, P., Brumt, C., Cook, C. S., Dubbert, M., Dyckmans, J., Gallagher, B., Gralher, B., Herbstritt, B., Hervé-Fernández, P., Hissler, C., Koeniger, P., Legout, A., Macdonald, C. J., Oyarzún, C., Redelstein, R.,
585 Seidler, C., Siegwolf, R., Stump, C., Thomsen, S., Weiler, M., Werner, C., and McDonnell, J. J.: Inter-laboratory comparison of cryogenic water extraction systems for stable isotope analysis of soil water. *Hydrol. Earth Syst. Sc.*, 22(7), 3619-3637, <https://www.doi.org/10.5194/hess-22-3619-2018>, 2018.
- Penna, D., Geris, J., Hopp, L., and Scandellari, F.: Water sources for root water uptake: Using stable isotopes of hydrogen and oxygen as a research tool in agricultural and agroforestry systems. *Agr Ecosyst Environ*, 291, 106790,
590 <https://www.doi.org/10.1016/j.agee.2019.106790>, 2020.
- Preisler, Y., Hölttä, T., Grünzweig, J. M., Oz, I., Tatarinov, F., Ruehr, N. K., Rotenberg, E., and Yakir, D.: The importance of tree internal water storage under drought conditions. *Tree Physiol*, 42(4), 771-783, <https://www.doi.org/10.1093/treephys/tpab144>, 2022.
- Rothfuss, Y. and Javaux, M.: Reviews and syntheses: Isotopic approaches to quantify root water uptake: a review and
595 comparison of methods. *Biogeosciences*, 14(8), 2199-2224, <https://www.doi.org/DOI.10.5194/bg-14-2199-2017>, 2017.
- Rothfuss, Y., Vereecken, H., and Brüggemann, N.: Monitoring water stable isotopic composition in soils using gas-permeable tubing and infrared laser absorption spectroscopy. *Water Resour. Res.*, 49(6), 3747-3755, <https://www.doi.org/10.1002/wrcr.20311>, 2013.
- Rothfuss, Y., Merz, S., Vanderborght, J., Hermes, N., Weuthen, A., Pohlmeier, A., Vereecken, H., and Brüggemann, N.: Long-
600 term and high-frequency non-destructive monitoring of water stable isotope profiles in an evaporating soil column. *Hydrol. Earth Syst. Sc.*, 19(10), 4067-4080, <https://www.doi.org/10.5194/hess-19-4067-2015>, 2015.
- Schmidt, M., Maseyk, K., Lett, C., Biron, P., Richard, P., Bariac, T., and Seibt, U.: Concentration effects on laser-based $\delta^{18}\text{O}$ and $\delta^2\text{H}$ measurements and implications for the calibration of vapour measurements with liquid standards. *Rapid Commun. Mass Spectrom.*, 24(24), 3553-3561, <https://www.doi.org/10.1002/rcm.4813>, 2010.
- 605 Seeger, S. and Weiler, M.: Dye-tracer-aided investigation of xylem water transport velocity distributions. *Hydrol. Earth Syst. Sc.*, 27(18), 3393-3404, <https://www.doi.org/10.5194/hess-27-3393-2023>, 2023.
- Sifton, H. B.: Air-Space Tissue in Plants .2. *Bot. Rev.*, 23(5), 303-312, <https://www.doi.org/10.1007/Bf02872447>, 1957.
- Sperry, J. S. and Love, D. M.: What plant hydraulics can tell us about responses to climate-change droughts. *New Phytol.*, 207(1), 14-27, <https://www.doi.org/10.1111/nph.13354>, 2015.
- 610 van Dusschoten, D., Pflugfelder, D., and Kochs, J.: Root water uptake in relation to plant transpiration, EGU General Assembly 2023, Vienna, Austria, 24–28 Apr 2023, EGU23-12018, <https://doi.org/10.5194/egusphere-egu23-12018>, 2023



- van Dusschoten, D., Kochs, J., Kuppe, C. W., Sydoruk, V. A., Couvreur, V., Pflugfelder, D., and Postma, J. A.: Spatially Resolved Root Water Uptake Determination Using a Precise Soil Water Sensor. *Plant Physiol.*, 184(3), 1221-1235, <https://www.doi.org/10.1104/pp.20.00488>, 2020.
- 615 Volkman, T. H. M., Kühnhammer, K., Herbstritt, B., Gessler, A., and Weiler, M.: A method for *in situ* monitoring of the isotope composition of tree xylem water using laser spectroscopy. *Plant Cell Environ*, 39(9), 2055-2063, <https://www.doi.org/10.1111/pce.12725>, 2016.
- von Freyberg, J., Allen, S. T., Grossiord, C., and Dawson, T. E.: Plant and root-zone water isotopes are difficult to measure, explain, and predict: Some practical recommendations for determining plant water sources. *Methods Ecol Evol*, 11(11), 1352-
620 1367, <https://www.doi.org/10.1111/2041-210x.13461>, 2020.
- Wassenaar, L. I., Hendry, M. J., Chostner, V. L., and Lis, G. P.: High Resolution Pore Water $\delta^2\text{H}$ and $\delta^{18}\text{O}$ Measurements by $\text{H}_2\text{O}_{(\text{liquid})}$ - $\text{H}_2\text{O}_{(\text{vapor})}$ Equilibration Laser Spectroscopy. *Environ. Sci. Technol.*, 42(24), 9262-9267, <https://www.doi.org/10.1021/es802065s>, 2008.
- Wei, C., Steudle, E., Tyree, M. T., and Lintilhac, P. M.: The essentials of direct xylem pressure measurement. *Plant Cell Environ*, 24(5), 549-555, <https://www.doi.org/10.1046/j.1365-3040.2001.00697.x>, 2001.
- 625 West, A. G., Patrickson, S. J., and Ehleringer, J. R.: Water extraction times for plant and soil materials used in stable isotope analysis. *Rapid Commun. Mass Spectrom.*, 20(8), 1317-1321, <https://www.doi.org/10.1002/rcm.2456>, 2006.
- Zhao, L. J., Xiao, H. L., Zhou, J., Wang, L. X., Cheng, G. D., Zhou, M. X., Yin, L., and McCabe, M. F.: Detailed assessment of isotope ratio infrared spectroscopy and isotope ratio mass spectrometry for the stable isotope analysis of plant and soil
630 waters. *Rapid Commun. Mass Spectrom.*, 25(20), 3071-3082, <https://www.doi.org/10.1002/rcm.5204>, 2011.



Appendix

Appendix A

RWU (expressed in ml water per time) at time t is the sum of three terms ($RWU_j, j = \{1; 2; 3\}$), i.e., the root water uptake from three *a posteriori* defined soil layers spreading respectively from 0-16.5 cm (top layer, encompassing the isotopically enriched water pulse), 16.5-36.5 cm (middle layer, encompassing the depleted water pulse), and 36.5-45 cm (bottom layer, where no labeled water was observed to enter):

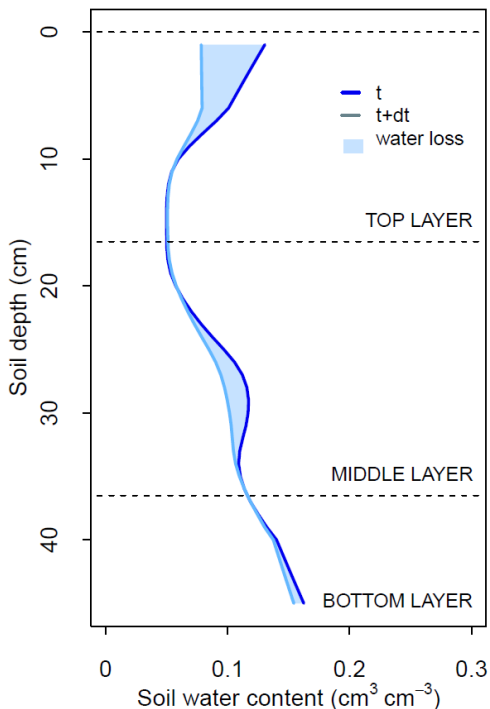
$$RWU(t) = \sum_{j=1}^3 RWU_j(t) \quad (A1)$$

$RWU_j(t)$ is calculated as the sum of the product between the soil slice volume (V , in cm^3 soil) and the difference in soil water content (SWC, cm^3 water cm^{-3} soil) measured in that particular slice between time t (dark blue curve in Fig. A1) and time $t+dt$ (light blue curve, Fig. A1) across slices i ($i = \{1; \dots; n\}$):

$$RWU(t) = \sum_{j=1}^3 RWU = \sum_{j=1}^3 \sum_{i=1}^n V_i \frac{[SWC_i(t+dt) - SWC_i(t)]}{dt} \quad (A2)$$

Note that $V_i = V_{\text{slice}} = \pi \left(\frac{\text{diameter}_{\text{slice}}}{2} \right)^2 \cdot \text{thickness}_{\text{slice}} = \pi \left(\frac{9}{2} \right)^2 \cdot 1 = 63.1 \text{ cm}^3$

RWU therefore equals the integral (represented as the blue-shaded area, Fig. A1) between the two SWC profile curves.



645 **Figure A1. Graphical illustration of the method for determining the plant total root water uptake (RWU, expressed in ml water per time) between time t and $(t+dt)$ on basis of the data collected by the Soil Water Profiler.**



Appendix B

650 Water ascending and flowing at rate Q_{RWU} (ml min^{-1}) in the xylem vessels (symbolized by the blue capillary in Fig. B1) exchanges with a given fraction of water (f_{ex} , -) contained in the stem (of volume V_{stem} , ml, colored in brown, Fig. B1).

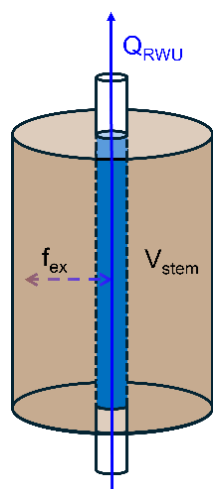


Figure B1. Graphical illustration of the stem water replacement model with xylem water.

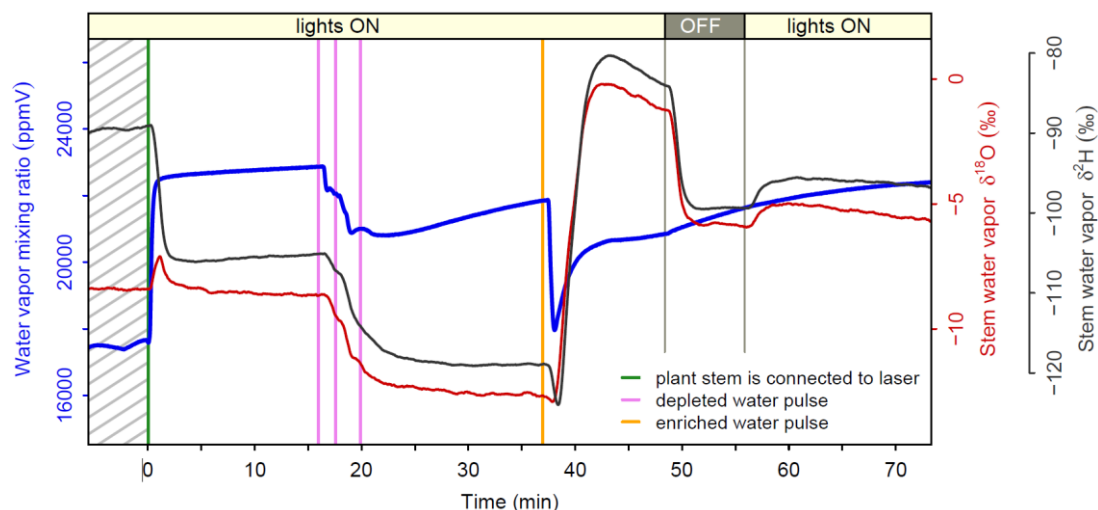
Appendix C

Hydroponic water solution	WVMR (ppmV)		$\delta^2\text{H}_{stem}^{vap}$		$\delta^{18}\text{O}_{stem}^{vap}$		$\delta^2\text{H}_{stem}$	$\delta^{18}\text{O}_{stem}$	$\delta^2\text{H}_b$		$\delta^{18}\text{O}_b$	
	mean	sd	mean	sd	mean	sd	$T_{water}=20^\circ\text{C}$		mean	sd	mean	sd
“Depleted” water (b1)	24487	9	-118.8	0.4	-13.5	0.3	-37.2	-3.7	-61.8	3.1	-13.6	1.3
	24431	8	-120.2	0.5	-13.7	0.2	-38.6	-3.9				
	24178	5	-116.7	0.5	-14.5	0.2	-35.1	-4.8				
Local tap water (b2)	24720	20	-113.6	0.5	-9.2	0.2	-32.0	0.6	-50.4	0.2	-7.4	0.1
	26234	11	-113.6	0.4	-9.9	0.2	-32.0	-0.2				
“Enriched” water (b3)	24232	31	-24.8	0.5	10.2	0.3	56.8	19.9	58.7	0.8	23.5	0.3
	23051	11	-29.9	0.6	9.8	0.3	51.7	19.6				
	23048	11	-24.0	0.6	11.2	0.3	57.6	21.0				

655 Table C1. Mixing ratio (WVMR) and isotopic composition (δ_{stem}^{vap}) values of the stem water vapor measured during the course of the calibration experiment, in which sunflower plants were grown in three different hydroponic solution water baths (designated as isotopically “depleted” water – b1, local tap water – b2, and “enriched” water – b3) at 20°C water temperature. The corresponding stem (liquid) water isotopic composition values, ($\delta^2\text{H}_{stem}$ and $\delta^{18}\text{O}_{stem}$) are reported as well. The ^2H - and ^{18}O -specific calibration functions were obtained by comparing the isotopic composition values in the water baths (i.e., δ_{b1} , δ_{b2} , and δ_{b3}) against the stem liquid water isotopic composition values averaged across the plants in each bath.



660 **Appendix D**



665 **Figure D1. Investigation of the response times in stem water vapor $\delta^2\text{H}$ (‰, black curve) and $\delta^{18}\text{O}$ (‰, red curve) of one individual plant following several “cold” labeling pulses (water temperature $\sim 10^\circ\text{C}$ versus soil initial water temperature $\sim 20^\circ\text{C}$) and following light intensity changes. The depleted and enriched water pulses were applied 16 and 37 minutes (see the violet and orange vertical lines) after connection of the plant stem to the laser spectrometer (as indicated by the green vertical line). LED lights were switched off 48 minutes after stem connection to the laser spectrometer and turned off again 7 minutes later.**

The response time, defined here as the difference between the time of perturbation (water addition via isotopic labeling or modification of light intensity) and the time of beginning of change of $\delta^2\text{H}$ or $\delta^{18}\text{O}$ was estimated between 20 and 30 seconds.

670 We note a fast decrease as well in water vapor mixing ratio (WVMR, ppmV, blue curve) after each consecutive labeling pulse (i.e., from 16-20 mins and 37-38 mins for the depleted and enriched labeling pulses, respectively) followed by a slower increase (20-37 and 38-48 mins, respectively). As per our hypothesis (see Sects 2.3 and 3.1), the collected stem air is water vapor-saturated, i.e., its WVMR is a (positive) function of temperature. Therefore, the observed dynamics in wvmr should be understood as due to a partial replacement of antecedent ($\sim 20^\circ\text{C}$) stem water with added and *colder* ($\sim 10^\circ\text{C}$) labeled water reaching the stem via root water uptake (RWU). As the temperature of the soil water (antecedent water + added water) increases again with time, so is its WVMR.

The changes in light intensity were strongly reflected by changes in stem water vapor $\delta^2\text{H}$ and $\delta^{18}\text{O}$ and less significantly by changes in WVMR (see 48-55 mins). We believe that switching off the lights incrementally stopped transpiration and shortly after RWU to occur. The contribution of the enriched water (rising inside the xylem vessels to the gas sampling location) to the water contained in all types of tissues in the stem section and that equilibrates with the hollow-space water vapor (see Fig. 5, 2nd case, panel c) therefore decreased. This translated isotopically into a decrease in both stem water vapor $\delta^2\text{H}$ and $\delta^{18}\text{O}$.

680 This is corroborated by a continuous increase in WVMR as the stem (water) temperature increased.



Appendix E

DoE begin	Time begin	DoE end	Time end	Top layer		Middle layer		Bottom layer	
				$\delta^2\text{H}$	$\delta^{18}\text{O}$	$\delta^2\text{H}$	$\delta^{18}\text{O}$	$\delta^2\text{H}$	$\delta^{18}\text{O}$
1	15:10	1	15:59	-47.7	-6.7	-50.4	-7.4	-50.4	-7.4
1	16:00	1	16:17	-6.5	4.2	-50.4	-7.4	-50.4	-7.4
1	16:18	1	16:59	17.0	10.5	-50.4	-7.4	-50.4	-7.4
1	17:00	2	09:44	38.8	16.2	-50.4	-7.4	-50.4	-7.4
2	09:45	2	10:05	38.8	16.2	-78.3	-11.1	-50.4	-7.4
2	10:06	2	10:15	38.8	16.2	-95.9	-13.5	-50.4	-7.4
2	10:16	2	13:50	38.8	16.2	-108.5	-15.2	-50.4	-7.4

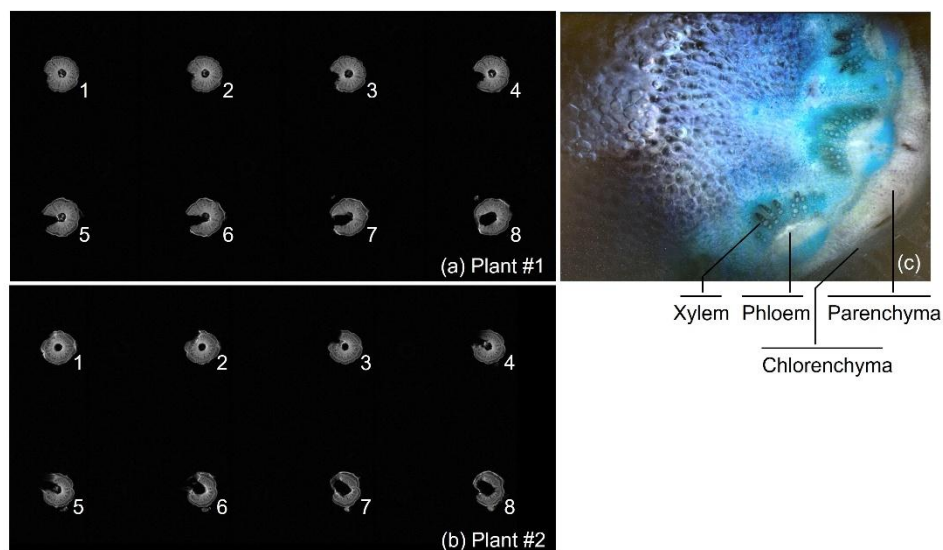
685 **Table E1.** Time evolutions of the simulated values of the (hydrogen and oxygen) isotopic compositions of soil water ($\delta_{\text{soil_sim}}$) in three layers (top: 0-16.5, middle: 16.5-36.5, and bottom: 36.5-45) used as input data for modeling of the isotopic composition of stem xylem water ($\delta_{\text{xyl_calc}}$, Sect. 2.4.4 and Sect. 3.3 of the main text) of plant #1. DoE stands for the day of experiment.

DoE begin	Time begin	DoE end	Time end	Top layer		Middle layer		Bottom layer	
				$\delta^2\text{H}$	$\delta^{18}\text{O}$	$\delta^2\text{H}$	$\delta^{18}\text{O}$	$\delta^2\text{H}$	$\delta^{18}\text{O}$
2	16:00	2	16:08	38.8	16.2	-108.5	-15.2	-50.4	-7.4
2	16:09	2	16:15	52.9	20.0	-108.5	-15.2	-50.4	-7.4
2	16:16	2	16:35	62.2	22.4	-108.5	-15.2	-50.4	-7.4
2	16:36	2	16:44	62.2	22.4	-121.6	-16.9	-50.4	-7.4
2	16:45	2	11:10	62.2	22.4	-129.1	-17.9	-50.4	-7.4

690 **Table E2.** Time evolutions of the simulated values of the (hydrogen and oxygen) isotopic compositions of soil water ($\delta_{\text{soil_sim}}$) in three layers (top: 0-16.5, middle: 16.5-36.5, and bottom: 36.5-45) used as input data for modeling of the isotopic composition of stem xylem water ($\delta_{\text{xyl_calc}}$, Sect. 2.4.4 and Sect. 3.3 of the main text) of plant #2. DoE stands for the day of experiment.



Appendix F



695 **Figure F1. Magnetic Resonance Imaging (MRI) pictures of the stems of plant #1 (panel a) and plant #2 (panel b).**

The MRI data shows holes significantly bigger than drilled, certainly a consequence of water vapor removal leading to dehydration of the inner stem. Eight 1.2 mm thick slices are shown (lowermost is number 1 and uppermost is number 8) for each plant. Panel c shows a microscopic observation (toluidine blue staining) of the peripheral part a plant stem section with a focus on the vascular bundles (xylem and phloem vessels).